

On the mechanisms of serrated airfoil trailing edge noise reduction

Mathieu GRUBER^a, Phillip F. JOSEPH^b

University of Southampton, ISVR, Tizard Building, Southampton, SO17 1BJ, UK

Tze Pei CHONG^c

Brunel University, Kingston Lane, Uxbridge, Middlesex, UB8 3PH, UK

This paper is an experimental investigation of the mechanisms involved in airfoil trailing edge noise reduction and noise increase observed by the introduction of sawtooth serrations at the trailing edge. This paper presents the results of an experimental campaign during which a set of over 30 sawtooth geometries were tested for noise on a NACA6512 airfoil. It is shown that the frequency above which noise is increased is fixed by a Strouhal number $St_\delta = f\delta/U_0 \sim 1$. It is also shown that, in the frequency region where noise is decreased, serrated trailing edges become an efficient means of noise radiation for $h/\delta > 0.5$ and reach a maximum efficiency when $h/\delta > 2$. In addition, the noise reduction improves when λ decreases. In other words, the sharper the serrations, the greater is the noise reduction. Hot wire velocity measurements reveal that these noise sources are located in the early wake, between the sawteeth of the serrated trailing edge, where small jets are forced through the troughs of the serrations. The results of this study are compared critically with Howe's theory. The noise reduction levels predicted by Howe are much greater than the measured ones, and the high frequency noise increase is not predicted. This work is relevant to reducing the noise from aircraft engines, aircraft wings, wind turbines and cooling fans. This work is supported by the 7th Framework European Project FLOCON and Rolls Royce plc.

I. Introduction

This paper is aimed at investigating the mechanisms of airfoil noise reduction obtained through the use of trailing edge serrations. Airfoil trailing edge noise is caused by the interaction between the turbulent structures in the boundary layer and the trailing edge discontinuity. Several researchers

^aPhD Student, Institute of Sound and Vibration Research, mg@isvr.soton.ac.uk, AIAA student Member.

^bProfessor, Institute of Sound and Vibration Research, pfj@isvr.soton.ac.uk, AIAA Member.

^cLecturer, University of Brunel, T.P.Chong@brunel.ac.uk, AIAA Member.

such as Ffowcs Williams & Hall,¹⁵ Amiet¹ and Howe^{9,12} for example, have shown that trailing edge noise radiation models can predict reasonably well experimental data measured in wind tunnels, using the unsteady surface pressure spectrum close to the trailing edge as an input. As trailing edge noise is a dominant source of noise in many aeronautical applications, various passive treatments for reducing trailing edge noise such as porous airfoils, brushes or serrated edges have been recently studied. This work focuses on trailing edge noise reduction using sawtooth serrations. It has been shown theoretically by Howe^{10,11} and experimentally by, for example, Parchen,¹⁴ Dassen,⁵ Oerlemans¹³ and Gruber *et al*^{7,8} that significant noise reductions are possible using such a geometry. It has also been reported in the experimental studies described in these papers that serrated edges provide a noise reduction in the lower and middle frequency regions but increases in noise at higher frequencies. Gruber *et al* has also shown that the frequency above which the radiated noise increases is Strouhal number dependent based on the boundary layer thickness at the trailing edge. Nevertheless, the mechanisms by which serrated edges affect noise radiation are still not understood. Howe^{10,11} proposes an analytical noise radiation model detailed in Section II, which is the only work that provides some insight about the physical mechanisms involved in the change of radiation efficiency when using serrated trailing edges.

This paper describes an experiment aimed at measuring the acoustic far field and the velocity near field around the airfoil trailing edge for the purpose of understanding the mechanisms of serrated trailing edge noise reduction. A short review of Howe's theory is given in Section II. The experimental setup is described in Section III. The noise radiation and aerodynamic results of the NACA6512 airfoil test campaign are presented in Sections V and VI, respectively. Section VII proposes a discussion on the noise mechanisms involved in the change of noise radiation introduced by sawtooth serrated trailing edges. This paper gathers experimental evidence that enhance the understanding of the mechanisms involved in the noise reduction performance of such trailing edge geometries. Results are compared to Howe's analytical solution and the hypothesis of his model are assessed against experimental data.

The reader is also referred to Gruber *et al*,⁸ in which complementary aerodynamic results in the boundary layer and in the wake of serrated trailing edges are described.

II. Howe's model for sawtooth trailing edges

A. Discussion and critique of Howe's theory of the noise from trailing edge serrations

Despite the potential of trailing edge serrations for providing significant reductions in trailing edge noise, only Howe appears to have analysed the problem analytically^{10,11}. It is not surprising that in a problem of this complexity, to make progress with an analytic solution, Howe made numerous approximations and simplifying assumptions. As is now well documented, Howe's final solution for the noise radiation from serrated trailing edges leads to a considerable over-estimate for the noise reduction compared with experimental data. Nevertheless, Howe's analysis provides useful insight into the mechanisms of noise reduction achievable through the use of trailing edge serrations. A critique of this paper is presented. Only restricted experimental data was available at the time

(1991) and so a critical comparison with data was not possible. This is the objective of the current work.

B. Mechanism of serrated trailing edge noise according to Howe

Howe argues that serrations applied to the trailing edge of an airfoil are able to reduce trailing edge noise by effectively reducing the spanwise length that contributes to sound generation. At sufficiently high frequency $\omega h/U_0$, only those components of wavenumber \mathbf{k} normal to the local edge (for which the trace phase speed along the edge is much higher than the sound speed) scatter efficiently into sound. This reduction in effective length occurs because at high frequency and low Mach number the dominant boundary layer contributions arise from $k_3/k_1 \sim 1$, where k_1 and k_3 are streamwise and spanwise boundary layer turbulence wavenumber components, respectively. Howe, therefore argues that trailing edge serrations with an angle greater than 45° to the flow direction are necessary to achieve good reductions in noise.

C. Mathematical developments

In this section we provide a short review of this theory and its limitations and then use it to predict the dependence of trailing edge noise on the main parameters. The starting point of Howe's theory is the Green's function solution given by Equation 1.

$$p(\mathbf{x}, \omega) = \int_S \int_{\mathbf{k}^3} p_b(\mathbf{K}) \gamma(K) [G(\mathbf{x}, \mathbf{y})] \exp(i\mathbf{k} \cdot \mathbf{y}) d^3 \mathbf{k} d\mathbf{y}, \quad (1)$$

$$\text{where } \gamma(K) = \begin{cases} \frac{\sqrt{\kappa^2 - K^2}}{i\sqrt{\kappa^2 - K^2}} & \text{for } K < \kappa \\ i\sqrt{\kappa^2 - K^2} & \text{for } K > \kappa \end{cases},$$

$\mathbf{K} = [k_1, 0, k_3]$ and $[G]$ is the jump in the Green function across the flat plate and a point in the far field whose normal derivative vanishes on the airfoil and p_b is the blocked pressure due to the boundary layer turbulence on one side, i.e., the pressure that would be produced by the turbulent flow on an infinite rigid plane wall.

D. Choice of Greens function

Whilst the choice of Greens function is essentially arbitrary, Howe chooses a Tailored Greens function appropriate to point sources close to a sharp trailing edge that is valid only at low frequencies at which the acoustic wavelength greatly exceeds the characteristic dimensions of the serration. His choice of Greens function is given by

$$G(\mathbf{x}, \mathbf{y}; \omega) = \frac{i\omega^{1/2} \sin(\theta/2) \sin^{1/2}(\alpha) \phi^*(\mathbf{y})}{\pi \sqrt{(2\pi c)} |\mathbf{x}|} \times \exp \left[i \left(\frac{\pi}{4} + \frac{\omega |\mathbf{x}|}{c} \right) \right], \quad \frac{\omega |\mathbf{x}|}{c} \gg 1, \quad (2)$$

where ϕ^* is a solution of Laplace's equation (for incompressible flow) that describes irrotational flow around the trailing edge. Howe then makes the important and restrictive assumption that the

serrations are shallow, i.e., $4h/\lambda \sim 1$ to allow the expression for ϕ^* to be used corresponding to a straight trailing edge ($h = 0$). The value of ϕ^* used in Howe's theory therefore represents an *upper bound* and his final expression for the level of noise reductions represents a *lower bound* value.

Following application of the method of stationary phase to evaluate this scattering integral, Howe makes the following conclusions:

- Only spanwise wavenumber contributions, $k_{3,n} = 2\pi n/\lambda$, contribute to far field sound radiation. This suggests that only wavenumber components matched to the trailing edge geometry radiate sound.
- For $\omega h/U_c \gg 1$, only streamwise wavenumber contributions satisfying $2\omega h/U_c = \pm n\pi$ contribute significantly to far field sound, i.e., wavenumber components arriving normally at the edge.
- The boundary layer pressure is dominated by streamwise wavenumber components in the convective region ω/U_c .

The final expression for the far field intensity is expressed in terms of a non-dimensional function whose behaviour is determined by the three non-dimensional parameters: $\omega\delta/U_c$, h/λ and h/δ .

We now assess the significance of the three terms to Howe's theory and comment on their physical effect on the radiated sound from serrated trailing edges. Comparison of these theoretical predictions with experimental data is then presented.

E. $\omega\delta/U_c$

In Howe's theory, frequency mostly appears in the combination $\omega\delta/U_c$, suggesting a Strouhal dependence based on boundary layer thickness. This is a feature of all boundary layer pressure spectral models and arises because δ controls the size of the largest eddys in the boundary layer while U_c/ω determines the characteristic hydrodynamic length scale. Howe predicts that noise reductions are largely independent of frequency for $\omega\delta/U_c > 1$, while negligible noise reductions and pressure increases are predicted for $\omega\delta/U_c < 1$. In our paper, we show that noise reductions are only achieved for $\omega\delta/U_c < 9$, with increases in noise being obtained for $\omega\delta/U_c > 9$. Note that the convection velocity was measured to be about $U_c = 0.7U_0$ on this airfoil.

F. h/λ

In Howe's model, serrat geometry enters the full expression through the ratio h/λ . Noise reductions are predicted to improve substantially as $h/\lambda \rightarrow \infty$, with comparatively small reductions being predicted for $h/\lambda < 0.2$. The principal reason for this effect, according to Howe's theory, is that as h/λ is increased, the boundary layer pressure at the wavenumbers, which arrive normally to the edge, reduces substantially. Moreover, as λ reduces the 'separation' between wavenumbers that satisfies this condition, $\Delta k_3 = 2\pi/\lambda$, increases and therefore there are less wavenumber contributions over the range of important wavenumbers to the radiated noise.

G. h/δ

For $h/\delta \sim 1$, the serration edge wetted by the turbulence is coherent leading to constructive and destructive interference between acoustic radiation generated at the root and at the tip. The spectrum of the radiated noise is therefore oscillatory with variations given by the term in Howe's theory, $\cos(2\omega h/U_c)$. For $h/\delta \gg 1$, only a part of the edge is coherent and hence radiation from the root and tip is incoherent and hence no oscillations are predicted in the radiated spectrum. In addition to this behaviour the predicted noise radiation appears to be weakly sensitive to h/δ (whilst keeping all other parameters fixed).

III. Experimental background and of the airfoil model

As part of the European project FLOCON, an experimental test campaign has been performed, aimed at reducing broadband trailing edge noise on a NACA6512 airfoil by the introduction of serrated trailing edges. The experiment was carried out in the ISVR's open-jet wind tunnel. A short overview of this facility, the airfoil model and the trailing edge treatments is given below.

A. The open-jet wind tunnel

The ISVR's open-jet wind tunnel is described in detail by Chong *et al.*^{3,4} Air is supplied from a centrifugal fan driven by a variable speed 110 kW motor. The maximum flow velocity in the test section is $M \approx 0.4$, before jet noise dominates over most of the frequency range. The dimensions of the nozzle exit are 0.45 m in width by 0.15 m in height. The jet has a turbulence intensity level of 0.4% at the airfoil leading edge. As seen in Figure 1, the nozzle is situated in the ISVR large anechoic chamber of dimensions 8 x 8 x 8 m. The use of side plates mounted flush with the nozzle exit maintains the flow two dimensionality and helps to support the test model horizontally.

Measurements of the far field noise are performed using a 20 B&K microphone array located at 1.2 m from the trailing edge (Figure 1). Microphones are placed at polar angles of between 40° and 135° .

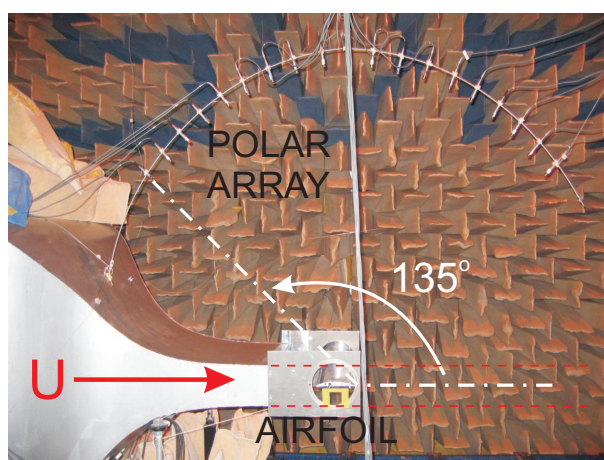


Figure 1. ISVR's open-jet wind tunnel showing the nozzle, the airfoil model and the polar array in the large anechoic chamber

B. In-jet airfoil test campaign

The airfoil model used for this study is a NACA6512-10 cambered profile with 0.15 m chord and 0.45 m span. It is typical of an airfoil used in turbomachinery and wind turbines applications. The airfoil has been designed and manufactured as part of the European project FLOCON as a baseline model for the investigation of trailing and leading edge noise reduction treatments. Figures 2a and b shows a photograph of the airfoil and an exploded view of the CAD drawing showing the different parts of the airfoil, respectively.

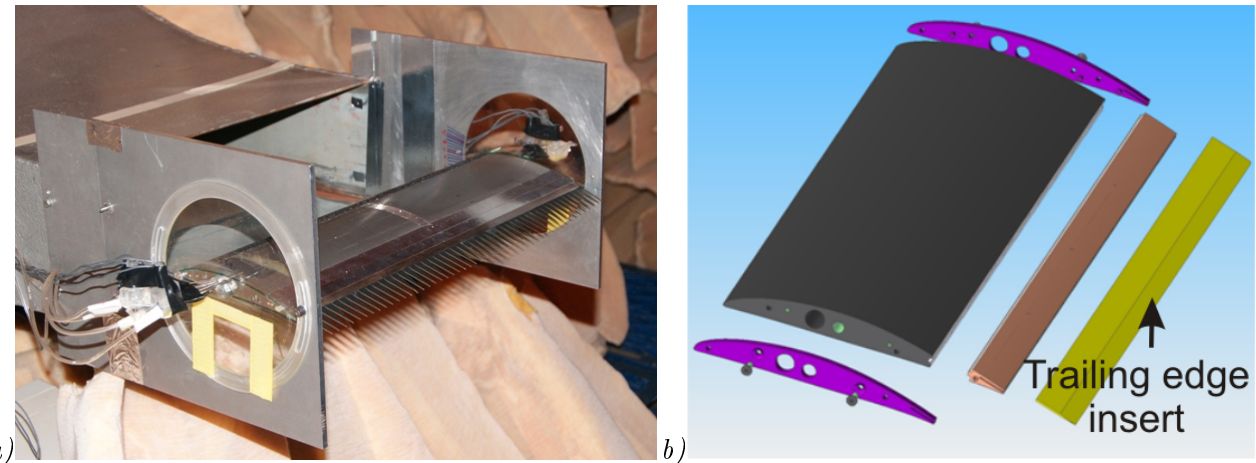


Figure 2. (a) NACA6512 airfoil with a sawtooth serrated trailing edge in the open-jet wind tunnel, (b) CAD exploded view of the NACA6512 airfoil model with a detachable trailing edge that allows flat plate straight and serrated edges to be inserted.

The test airfoil is composed of a main steel body of 0.1 m in length and a detachable trailing edge, 0.05 m in length, which allows flat plate serration geometries to be inserted at the airfoil trailing edge. Capillary tubes of 0.6 mm external diameter are connected to the surface in the mid-span plane and run along the span of the airfoil allowing measurements to be taken of the static and unsteady pressure for all trailing edge geometries. As shown in Figure 2a and b, trailing edge serrations are cut into thin flat plates and inserted into the airfoil. All inserts are made of rigid cardboard of thickness 0.8 mm. This process of attachment avoids any bluntness at the root of the serrations that result in vortex shedding and hence strong tones in the far field noise spectra. A straight unserrated edge made of the same material is used as the baseline configuration for all tests. The baseline straight edge configuration, for a given sawtooth geometry, is defined to have the same total airfoil area, thus giving the same effective wetted airfoil surface and minimizing any effects due to changes in total lift.

Measurements with identical airfoil trailing edge insert geometries made of steel and cardboard were performed and showed no significant difference in the radiated noise spectrum. Cardboard was chosen for ease of manufacturing and allowed 36 sawtooth serrated edges to be designed and laser cut. Two geometrical parameters h and λ were varied, respectively corresponding to half the root to tip distance and the periodicity, as shown in Figure 3a.

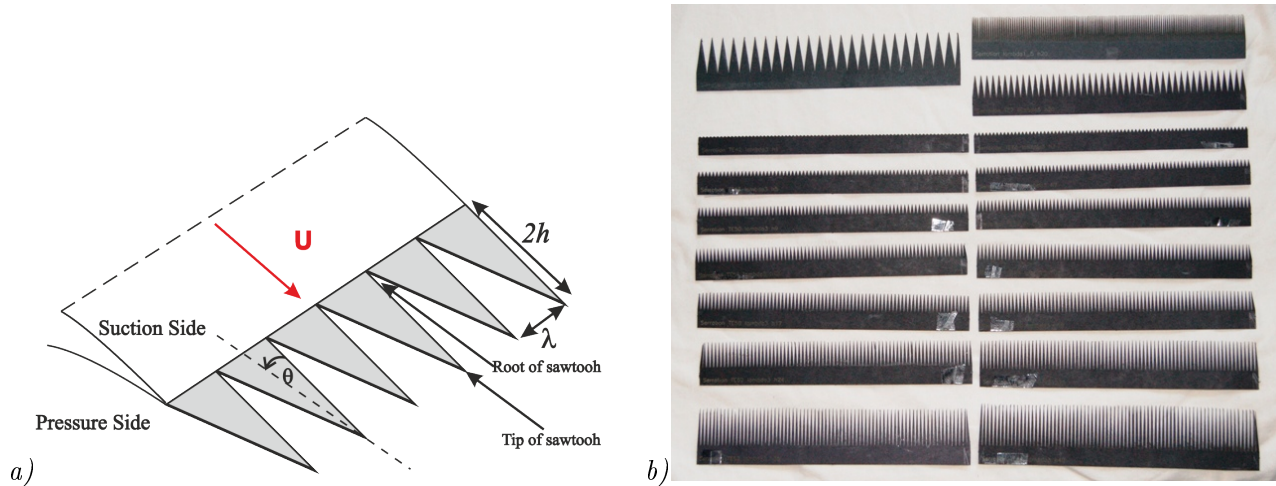


Figure 3. (a) Sketch of a sawtooth serrated edge with study parameters h and λ , (b) Photograph showing a sample of the serrated trailing edge inserts manufactured with a laser cutter.

Noise data were recorded at the four mean flow velocities of 20, 40, 60 and 80 m/s ($Re_c=206,500$, 413,000, 620,000 and 826,000 respectively) and for the two geometrical angles of attack $\alpha_g = 0$ and 5° . Note that to compensate for the jet deflection by the airfoil at non zero angles of attack, the angle of attack correction given by Brooks *et al*² was applied to evaluate the effective angles of attack in free air α_e . The geometrical angle of attack α_g in the rig is defined as the angle between the flow and the chord line. Note that to ensure fully developed turbulence in the boundary layer at lower Reynolds number, the airfoil was tripped at $x/c = 0.2$ using a rough band of tape on both suction and pressure sides.

IV. Estimation of the boundary layer parameters using Xfoil

As suggested in Howe's theory,¹¹ the boundary layer thickness δ at the airfoil trailing is an important parameter in determining the noise performance of trailing edge serrations. To estimate the boundary layer thickness, the turbulent boundary layer profile was measured experimentally at various locations along the baseline airfoil chord, at $U_0 = 40\text{m/s}$ and 5° AoA, using a single wire probe. For simplicity and because of the large number of cases in this study, Xfoil⁶ was used to estimate the boundary layer parameters at any location along the chord and any mean flow velocity. In order to relate Xfoil with the experiment, the deflection of the flow due to the high camber of the airfoil and the geometrical angle of attack in the rig, was taken into account. This was done by adjusting the angle of attack predicted by Xfoil so that the static pressure distribution along the airfoil chord, on the suction side, matches with the RANS calculation provided by FLUOREM (using theTurb'opt software) and the experimental data (Figure 4a). Figure 4b shows good accuracy in the estimation of the boundary layer displacement thickness by Xfoil when compared with experimental data, at 99% of the chord on the suction side. Therefore, by matching the static pressure distribution, Xfoil⁶ was used to estimate the boundary layer thickness data in this study for all cases, angles of attack and flow speeds.

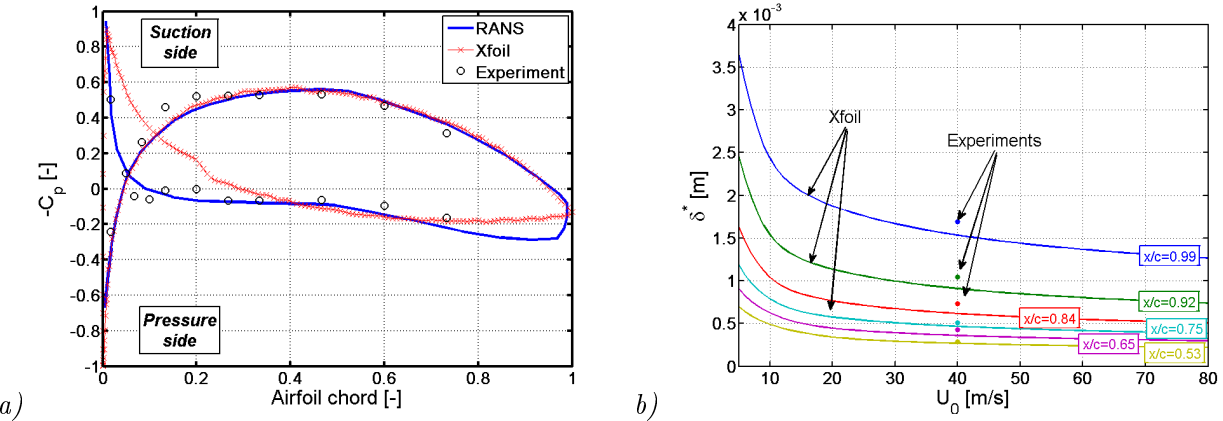


Figure 4. (a) Static pressure distribution along the airfoil chord at 5° angle of attack, (b) Estimation of δ^* as a function of mean flow velocity at various position along the airfoil chord using Xfoil.⁶

V. Noise radiation from a sawtooth serrated trailing edge

As presented by, for example, Dassen *et al.*,⁵ Parchen *et al.*,¹⁴ Gruber *et al.*,⁸ serrated edges have been used as means of reducing trailing edge self noise in airfoil wind tunnel tests and for wind turbine applications, in Oerlemans *et al.*.¹³ All of these studies have consistently shown noise reductions of up to 5 dB over large frequency bands but an increase of noise at higher frequencies. As described in Section II, Howe¹¹ provides useful insights into the important parameters that, under the numerous assumptions made to develop his model, determine noise reduction due to sawtooth trailing edges. The ratio of the sawtooth amplitude over the boundary layer thickness, h/δ , controls the oscillatory behaviour of the far field pressure spectrum due to coherent or incoherent radiation of the noise sources distributed along the wetted edges. The serrat geometry, introduced as h/λ , sets the minimum noise reduction level achievable for a given geometry, where the noise reduction increases as $h/\lambda \rightarrow \infty$. Finally, $\omega\delta/U_c$ controls the frequency range over which noise reduction is independent of frequency. More specifically, for $\omega\delta/U_c > 1$ noise reductions are predicted to be independent of frequency while for $\omega\delta/U_c < 1$ the noise reduction is insignificant. The main parameters controlling the noise reduction levels and frequency range are therefore predicted to be h/λ and $\omega\delta/U_c$, respectively.

Howe also predicts that the angle θ , given in Figure 3 as the angle between the flow and the wetted edges of the sawtooth, has to be less than 45° for the sawtooth to reduce the noise radiation. In this study, all serrated geometries satisfy the condition $\theta < 45^\circ$ (equivalent to $h/\lambda > 0.2$ using notations of Figure 3), and therefore this prediction cannot be tested in this experimental investigation.

This section describes the experimental noise performance of the sawtooth serrated geometries measured in the ISVR open-jet wind tunnel. Note that the convection velocity, measured to be about $U_c = 0.7U_0$ on this airfoil, is used when using Howe's model to predict the theoretical noise reductions matched to the experimental data.

A. Variation of sound power level (PWL) with varying λ

This Section investigates the variation of radiated sound power level with varying sawtooth periodicity λ . Assuming cylindrical radiation, the sound power level PWL , per unit span, is given in Equation 3 and measured between radiation angles of 50° and 110° .

$$PWL = 10 \log_{10} \sum_i \left(\frac{Lr}{\rho c_0} \frac{S_{pp}(\theta_i) \cdot \Delta\theta}{10^{-12}} \right) , \quad i = 1, \dots, N \quad 50^\circ < \theta < 110^\circ , \quad (3)$$

where $S_{pp}(\theta_i)$ is the PSD measured at microphone i , N is the number of microphones, L is the airfoil span, r is the distance between the airfoil trailing edge and the observer and c_0 is the speed of sound. Figure 5 shows a comparison of the sound power PWL measured at 5° angle of attack and $U_0 = 40 \text{ m/s}$, for the nine serrated edges given in Table 1 relative to that of a straight edge of identical wetted surface area. Data are presented over the low and mid frequency bandwidth 300 Hz to 7 kHz (Figure 5a and c), and over the high frequency bandwidth 7 kHz to 20 kHz (Figure 5b and d).

$h = 10$	$\lambda = 1.5$	$\lambda = 3$	$\lambda = 5$	$\lambda = 8.5$	$\lambda = 19$
$h = 15$	$\lambda = 1.5$	$\lambda = 3$	$\lambda = 7$	$\lambda = 12.5$	-

Table 1. Sawtooth serration geometries as in Figure 5. All dimensions are given in millimetres

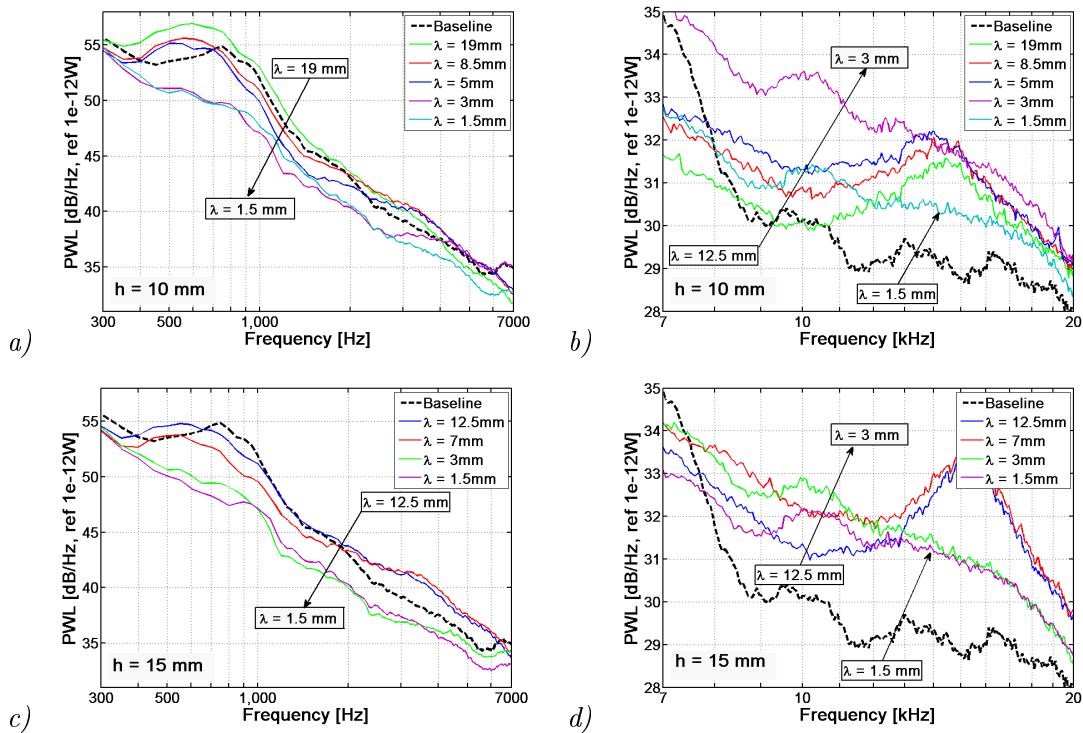


Figure 5. Measured far field power spectrum showing a comparison between baseline unserrated edge and serrated edges for various values of λ and two values of h - Airfoil at 5° AoA and $U_0 = 40 \text{ m/s}$ - (a) $h = 10 \text{ mm}$ from 300 Hz to 7 kHz, (b) $h = 10 \text{ mm}$ from 7 kHz to 20 kHz, (c) $h = 15 \text{ mm}$ from 300 Hz to 7 kHz, (b) $h = 15 \text{ mm}$ from 7 kHz to 20 kHz.

Figure 5*a* shows that at lower frequencies, below 400 Hz, noise reductions limited to 1 dB are obtained due to the dominance of jet noise. For $\lambda = 1.5 \text{ mm}$ and $\lambda = 3 \text{ mm}$, a maximum noise reduction of about 5 dB is obtained in the mid frequency range. Generally, the noise reduction is increased as λ is reduced. As shown in Figure 5*c*, a similar behaviour is observed for a larger amplitude of $h = 15 \text{ mm}$, with a larger maximum reduction of 7 dB for $\lambda = 1.5 \text{ mm}$. Figures 5*b* and *d* show an increase in the sound power PWL at high frequencies, for all values of λ , which increases with decreasing λ . The power increases by a maximum of about 3 dB for all cases.

Figure 5 shows that, given the flow conditions of this study, sawtooth serrations are most effective at reducing the radiation efficiency in the mid frequency range, while for higher frequencies, the sound power increases with decreasing λ . This increase in the noise radiation using serrations at the airfoil trailing edge was reported in previous studies, as mentioned in Section V. Oerlemans¹³ observed that a misalignement of the serrations with the flow direction causes this increase in noise. This observation is consistent with the presence of cross flow through the root of the serrations. This hypothesis is verified in Section VI from hot wire data.

Equation 4 defines the difference in sound power level ΔPWL , between a sawtooth trailing edge and a straight trailing edge airfoil, where $S_{pp,serr}(\theta_i)$ is the PSD measured at microphone i for a serrated trailing edge, $S_{pp,ref}(\theta_i)$ is the reference PSD measured at microphone i for the straight edge baseline airfoil, and N is the number of microphones.

$$\Delta PWL = 10 \log_{10} \left(\frac{\sum_i S_{pp,serr}(\theta_i)}{\sum_i S_{pp,ref}(\theta_i)} \right), \quad i = 1, \dots, N, \quad 50^\circ < \theta < 110^\circ, \quad (4)$$

Figures 6*a* and *b* show ΔPWL , as given above, versus λ/δ , averaged over the low frequency bandwidth 1 kHz to 2 kHz, and over the high frequency bandwidth 10 kHz to 12 kHz, respectively. The results are shown together for the angles of attack 0° , 5° and 10° , and mean flow velocity for $h = 10 \text{ mm}$ (circles) and $h = 15 \text{ mm}$ (squares). Note that λ is non-dimensionalised by the boundary layer thickness δ in order to compare data from both sawtooth amplitudes $h = 10 \text{ mm}$ and $h = 15 \text{ mm}$, as was previously presented in Figure 5.

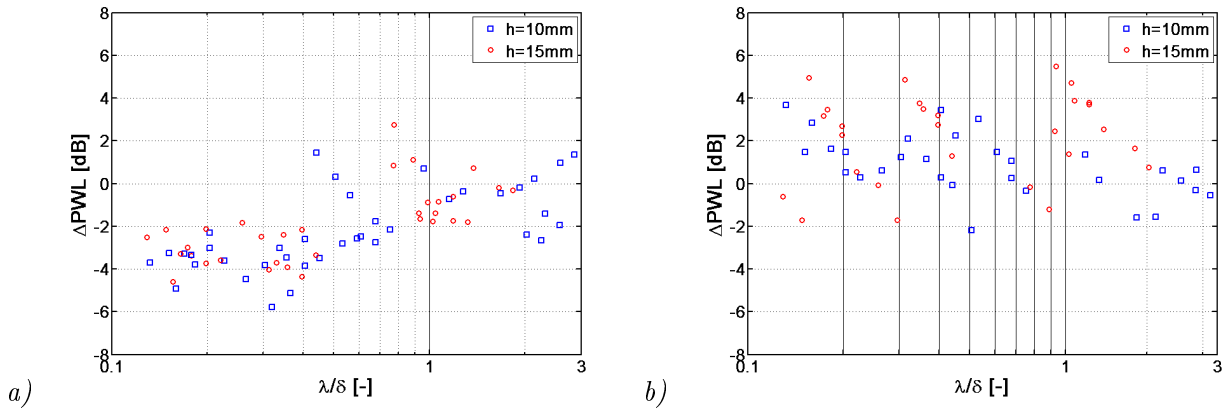


Figure 6. Scattering of measured ΔPWL as a function of λ/δ - Data include variation over mean flow velocity ($U_0 = 20, 40, 60 \text{ m/s}$), AoA ($0^\circ, 5^\circ$ and 10°) for two amplitude serrations $h = 10\text{mm}$ (square) and $h = 15\text{mm}$ (circle) - (a) ΔPWL averaged between 1 and 2 kHz, (b) ΔPWL averaged between 10 and 12 kHz.

Figure 6a shows maximum sound power reductions of between 4 and 6 dB as λ/δ decreases. Figure 6b emphasizes that for the high frequency range, the radiated power is increased by up to 6 dB as λ/δ decreases. Generally, Figures 6a and b confirm that decreasing λ causes an increase of noise reduction at low to mid frequencies and a decrease of noise reduction at higher frequencies. The data presented in Figures 6a and b also contain a large amount of scatter and no obvious trends can be drawn with respect to angle of attack, mean flow velocity or sawtooth amplitude h . Figure 10 also later shows a scattering of ± 1 dB in the experimental sound power data. A detailed investigation of the effect of h on noise reduction is presented in Section C.

Figures 7a and b show the pressure difference ΔSPL (as given in the caption) predicted by Howe's model, over the low frequency bandwidth 1 kHz to 2 kHz, and over the high frequency bandwidth 10 kHz to 12 kHz, respectively. It is presented as a function of λ/δ with all parameters chosen to match the experiment (same flow conditions and sawtooth geometries as presented in Figure 6). Note that the theoretical predictions by Howe are given in terms of sound pressure level ΔSPL , hence exact comparisons of the magnitudes between Figures 6 and 7 is not appropriate. However, the differences are large enough (>10 dB) to suggest that the theoretical noise reduction predictions are unrealistically high.

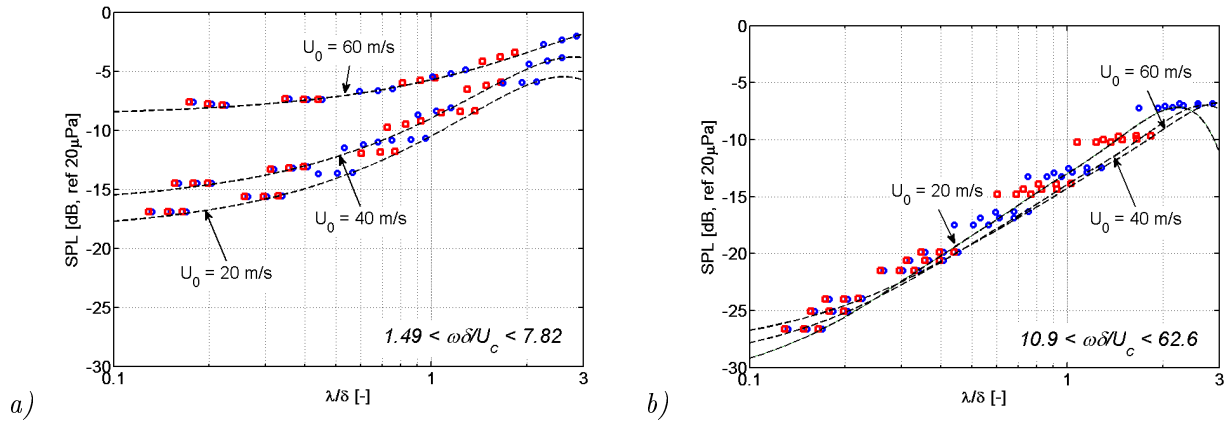


Figure 7. Variation of sound pressure difference $\Delta SPL = 10 \log_{10} (Spp_{serr}/Spp_{ref})$ using Howe's formulation as a function of λ/δ - Data include variation over mean flow velocity ($U_0 = 20, 40, 60$ m/s) and boundary layer thickness δ , for two amplitude serrations $h = 10$ mm (square) and $h = 15$ mm (circle) - (a) ΔSPL averaged between 1 and 2 kHz, (b) ΔSPL averaged between 10 and 12 kHz.

Figure 7a shows that the theoretical noise reduction increases with decreasing λ , at a much higher rate than the measured noise reductions, giving a maximum noise reduction of 18 dB at 20 m/s and of 8 dB at 60 m/s. As δ is only used as a normalisation parameter on λ in Figure 7, the change in rate with which noise reduction is increased in Figure 7a can be directly related to the parameter $\omega\delta/U_c$ through a measured value of $U_c = 0.7U_0$. A direct comparison of Figures 7a and b, confirms that when $\omega\delta/U_c$ decreases and gets closer to unity, the far field noise reduction becomes less and less significant relative to that of a straight edge. Figure 7b also shows that for sufficiently high values of $\omega\delta/U_c$, the noise reduction collapses for a given frequency range and for a range of mean flow velocities and for two sawtooth amplitudes. Finally, Figure 7b also shows that the experimental noise increase observed in Figures 5 and 6, and reported in various other studies, is not predicted by Howe's model.

B. Variation of PWL with mean flow velocity

This section is dedicated to the investigation of the changes in sound power radiation with varying mean flow velocity. The boundary layer thickness is directly related to the mean flow velocity as shown in Figure 4. For a given mean flow velocity U_0 and boundary layer thickness δ , Gruber *et al*⁸ reported that $St_\delta = f_\delta \delta / U_0 \sim 1$ gave a good estimate of the frequency f_δ above which the noise is increased.

Figure 8 shows the typical behaviour of the sound power level reduction ΔPWL , defined in Equation 4, as a function of frequency and mean flow velocity U_0 . Note that the limits of ± 2 dB are set manually to emphasize the behaviour of the transition frequency between power reduction and power increase and do not refer to maximum and minimum changes in power.

By inspection of these maps, the frequency delimiting noise reductions and noise increases appear to closely follow a constant Strouhal number dependency where $St_\delta \sim 1$, as mentioned previously. Figure 8 suggests that St_δ varies with angle of attack and sawtooth geometry by less than 20 % around a value approximately equal to 1. The general trend over the whole set of sawtooth trailing

edges, not shown here for brevity, suggests that $St_\delta \sim 1$. We speculate that the variation of St_δ observed in Figure 8, from 0.7 to 1.2 is partly due to variations in boundary layer thickness over the sawtooth, not taken into account using Xfoil.⁶ This was demonstrated by Figures 14 and 15 in Gruber *et al*⁸ where measurements of the mean and turbulent streamwise velocity over a single sawtooth are compared with respect to a baseline straight edge.

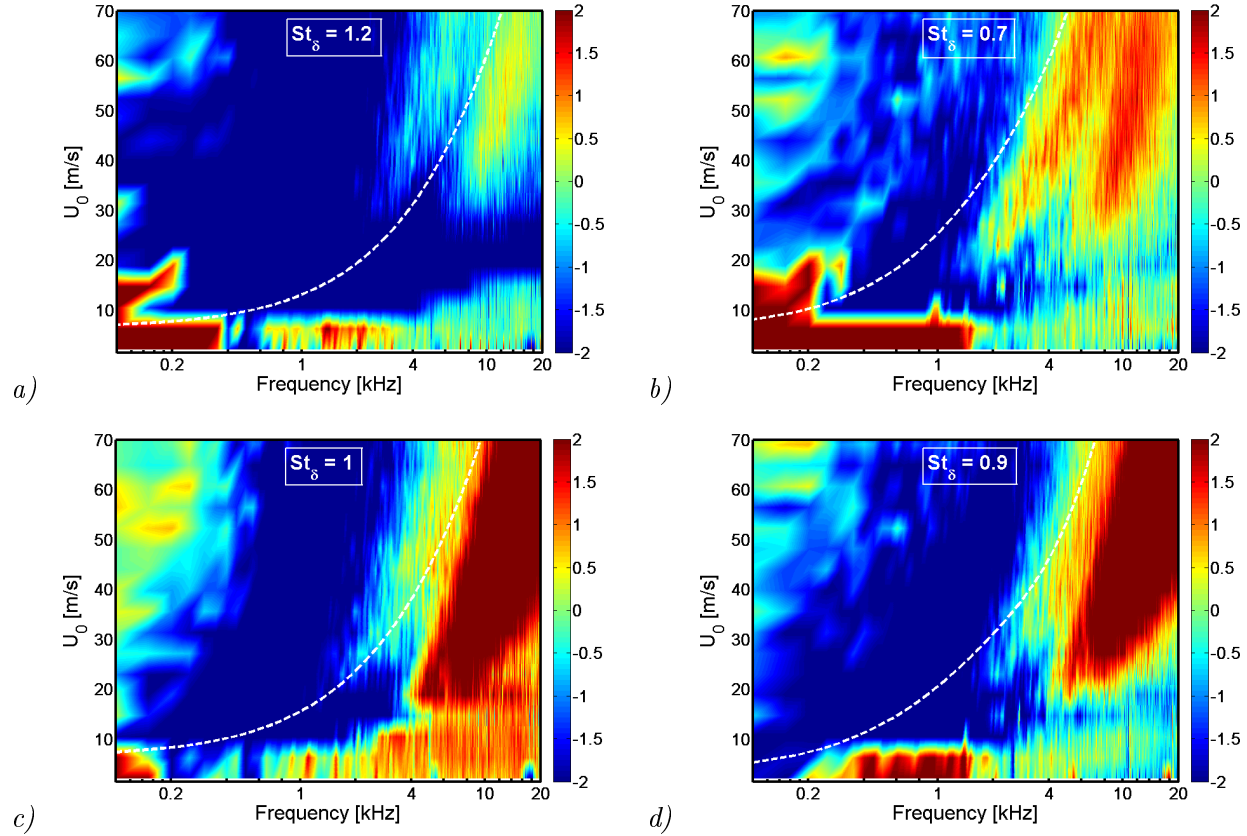


Figure 8. Sound power level reduction ΔPWL as a function of frequency and mean flow velocity U_0 , (a) Serration $\lambda = 9\text{mm}$, $h = 15\text{mm}$ - 0° AoA, (b) Serration $\lambda = 9\text{mm}$, $h = 15\text{mm}$ - 5° AoA, (c) Serration $\lambda = 3\text{mm}$, $h = 15\text{mm}$ - 0° AoA, (d) Serration $\lambda = 3\text{mm}$, $h = 15\text{mm}$ - 5° AoA.

C. Variation of PWL with sawtooth amplitude $2h$

The purpose of this section is to investigate the importance of the root-to-tip distance $2h$, (also denoted '*amplitude*' of the sawtooth) in the noise reduction efficiency of sawtooth serrations. This was undertaken using 27 sawtooth inserts of gradually increasing amplitude from 1 mm to 40 mm, corresponding to a total baseline chord of 0.14 m to 0.16 m, respectively (chord line based on the same airfoil wetted area between a straight edge and a serrated edge), while keeping the periodicity λ fixed and equal to 3 mm. As in Section A, and in order to compare the experimental data with Howe's theory, the boundary layer thickness δ was used as a normalisation parameter on h . Using Xfoil as described in Section IV, and for each value of h , δ is estimated at 99 % of the chord on the corresponding baseline straight edge airfoil. Although it was proved by Gruber *et al*⁸ that the boundary layer thickness changes due to the sawtooth trailing edge, it is assumed for simplicity that

δ remains unchanged by the presence of the sawtooth. Similarly, Howe uses the same assumption and also introduces h/δ as a parameter controlling the coherent or incoherent radiation of the sources along the wetted edges.

Figure 9 shows the difference in sound power level ΔPWL , in third octave bands averaged between 50° and 110° , given by Equation 4. The power reduction ΔPWL is shown as a colormap as a function of Strouhal number $f\delta/U_0$, h/δ , and h/λ . Data is given for the angles of attack of 0° and 5° , and for velocities of 20 m/s, 40 m/s, 60 m/s and 80 m/s. Note that the limits of $+/- 2dB$ are set manually to emphasize the behaviour of the transition frequency between power reduction and power increase and do not refer to maximum and minimum changes in power.

Figure 9 shows clearly that for both angles of attack and all mean flow velocities, noise reductions occur only in the low frequency range for $f\delta/U_0 < St_\delta$, where $St_\delta \sim 1$ and noise increase occur when $f\delta/U_0 > St_\delta$. As mentioned in Section B, $St_\delta \sim 1$ varies by no more than 30 % depending upon serration geometry and AoA, as shown by the vertical dashed line. Note that St_δ seems to decrease with increasing mean flow velocity. A part of this variation is believed to be due to the error in the estimation of the boundary layer thickness using Xfoil. The other striking feature of Figure 9 is that sawtooth serrations are inefficient at reducing noise radiation when the root to tip distance is less than half the boundary layer thickness. In general, it seems that for $h/\delta \sim 0.5$ the sawtooth serration is efficient over a frequency band $0.5 < f\delta/U_0 < 1$. Figure 9 reveals a critical value of either $h/\delta \sim 0.5$ or $h/\lambda \sim 1$, above which significant noise reductions occur. However, Howe's theory (see Figure 11) and common sense suggest that noise reductions should vary smoothly with h/λ and therefore can be discounted as the cause of this sudden increase in noise reduction. Consequently, it is much more plausible that this behaviour arises from the critical value of $h/\delta \sim 0.5$, below which the eddys are too large to be influenced by the amplitude h of the serration. Further discussions about the relative importance of h/δ and h/λ are presented in Section VII.

For longer serrations $0.5 < h/\delta < 2$, the noise reduction spreads to lower frequencies $0.01 < f\delta/U_0 < 1$. Little differences are observed between the two angles of attack 0 and 5° . This behaviour is not predicted by Howe's model, which suggests that either his model breaks down for the range of parameters under investigation or another source is present that is not included in Howe's model. Generally, the parameter h/λ does not introduce any striking feature in the sound power level difference and, in contrast with Howe's theory, its relevance relative to h/δ needs to be reconsidered.

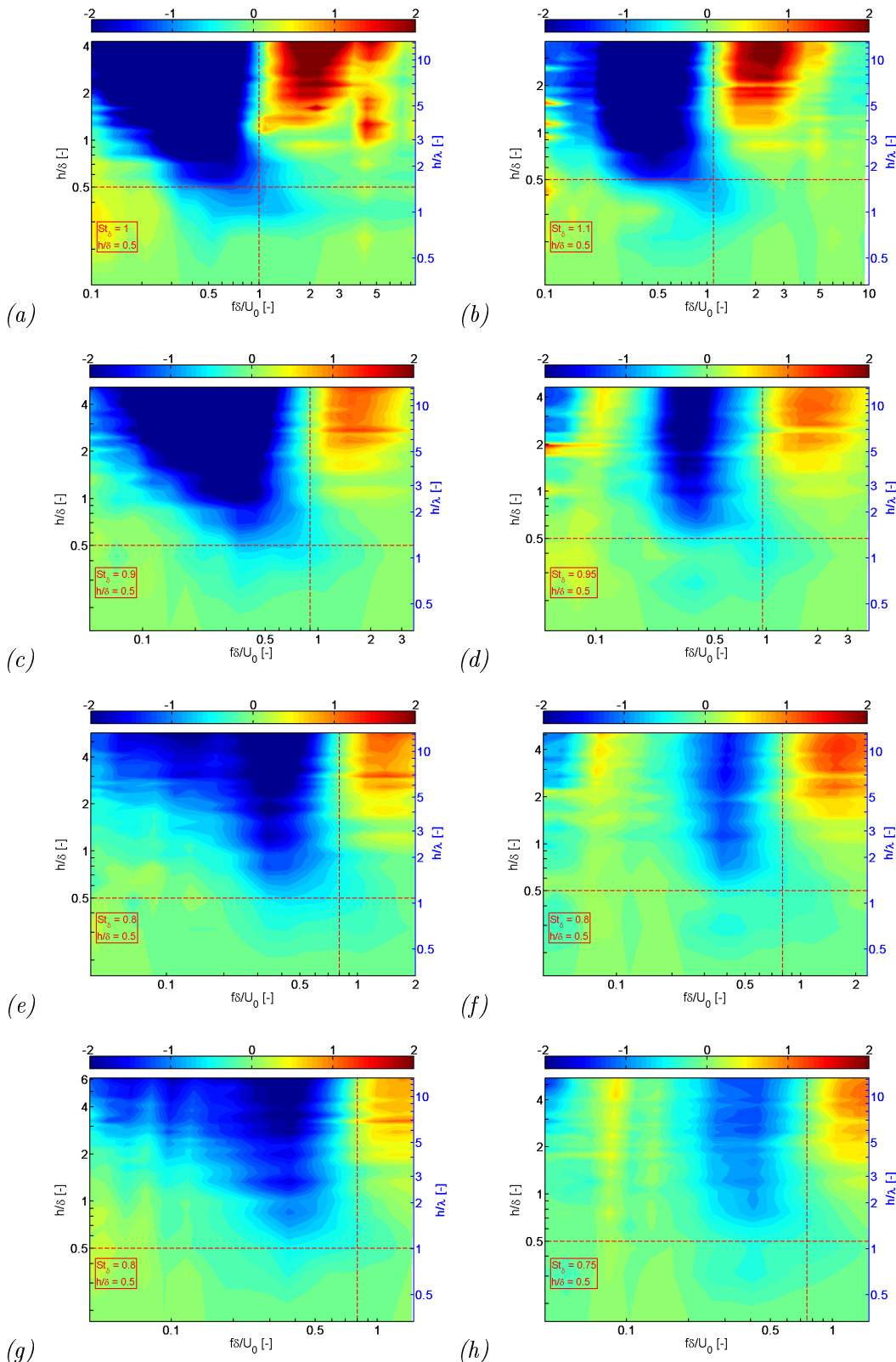


Figure 9. Sound power level difference $\Delta OASWL$ as a function of $f\delta/U_0$ and h/δ , (Left) 0° AoA, (Right) 5° AoA, (From top to bottom) $U_0 = 20, 40, 60$ and 80 m/s.

Figure 10 is a plot of ΔPWL plotted in Figure 9, as a function of h/δ , for the four third octave bands 1 kHz, 3.15 kHz, 5 kHz and 10 kHz, and for the four mean flow velocities $U_0 = 20, 40, 60$ and 80 m/s. It is shown in order to illustrate the dependence on h more clearly. Indeed, as mentioned previously, Figures 10 *a* to *d* illustrate Figure 9 in that for $St_\delta < 1$ (Dashed lines) the radiation efficiency decreases due to the sawtooth trailing edges, while increasing when $St_\delta > 1$ (Solid lines), over the whole frequency range. Similarly, when $h/\delta < 0.5$ the sawtooth serrations are inefficient at reducing the power radiation. For most cases of sawtooth amplitudes satisfying $h/\delta > 0.5$, the noise radiation efficiency decreases with increasing h/δ . These observations confirm Howe's theory in the sense that the sharper the sawtooth, the greater is the noise reduction. Similarly, at higher frequencies when $St_\delta > 1$, the increase in sound power radiation due to the sawtooth trailing edges increases with increasing h/δ . Note that although the trends described above are clearly shown in Figure 10, locally the sound power data deviates by up to ± 1 dB from the tendency. This is believed to explain part of the large scattering of the data seen in Figure 6.

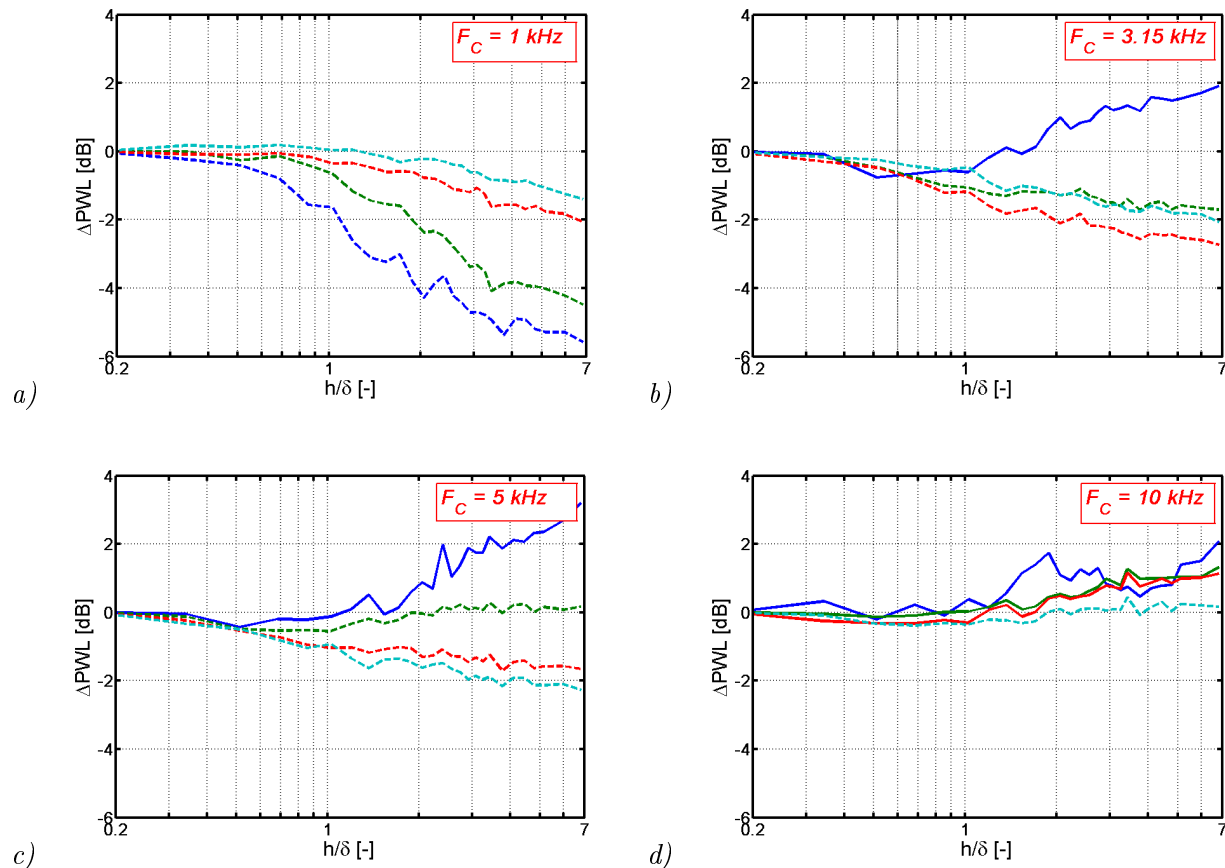


Figure 10. Sound power level difference ΔPWL as a function of h/δ at 0° AoA - (Solid) $f\delta/U_0 > 1$, (Dashed) $f\delta/U_0 \leq 1$ - (a) Third octave band 1 kHz, (b) Third octave band 3.15 kHz, (c) Third octave band 5 kHz, (d) Third octave band 10 kHz.

Figure 11*a* presents the difference in sound pressure level using Howe's prediction model for sawtooth trailing edges. The data is shown as a function of Strouhal number $f\delta/U_0$, h/δ , and h/λ , for $U_0 = 40 \text{ m/s}$ and 0° angle of attack. In order to compare Howe's theory with the experimental

data, Figure 11b reproduces the map of Figure 9c, for which the flow conditions are identical. In addition, as was shown previously, Howe's model does not predict the increase in noise for $f\delta/U_0 > 1$, hence both Figures 11a and b are only presented for $f\delta/U_0 \leq 1$. A direct comparison shows that the decrease in radiation efficiency with increasing h/δ , shown in the measured data, begins in Howe's theory for $f\delta/U_0 > 0.2$. The important condition for a decrease in noise radiation shown experimentally, $h/\delta > 0.5$, does not appear in Howe's model. Generally, the condition $h/\delta = 0.5$ does not appear to be a critical value in Howe's model.

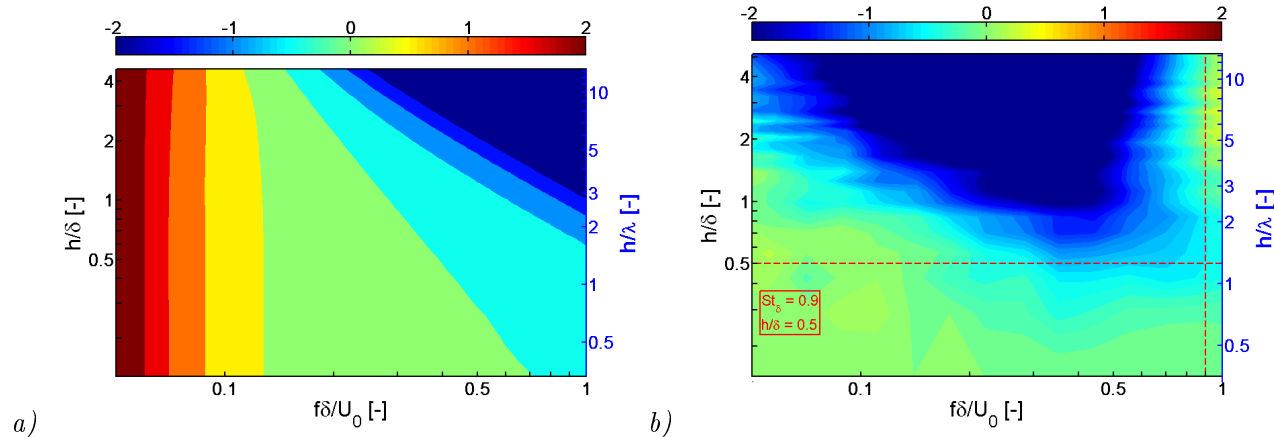


Figure 11. (a) Sound pressure level difference from Howe's theory and (b) from measured data as a function of $f\delta/U_0$ and h/δ at $U_0 = 40$ m/s and δ for 0° AoA.

VI. Flow around a sawtooth serrated airfoil trailing edge

As mentioned in Section V, although sawtooth trailing edges are an effective means of reducing the far field noise in the low to mid frequency range, the noise radiation at high frequency is consistently increased. This was also previously reported and attributed to a possible misalignment of the sawtooth trailing edge with the flow. This phenomenon is not predicted by Howe's analytical model.¹¹ In this paper, it is believed that an extraneous source of noise due to a cross flow through the troughs of the sawtooth, generates this increase in the high frequency radiation levels.

This section reports an experiment aimed at visualising the cross flow phenomenon in the vicinity of the trailing edge, and also presents hot wire measurements of the streamwise boundary layer and very near wake velocity spectra on a sawtooth and a straight edge airfoil.

A. Sawtooth serration cross flow

This section is dedicated to visualising and qualitatively analysing the flow over a straight and a serrated trailing edge. Flow visualisation was performed using a smoke wand generating a point source of smoke to understand the behaviour of the flow in the close vicinity of the serration. The mean flow velocity was $U_0 = 40\text{m/s}$ and the airfoil angle of attack was 5° , for a serration with $2h = 20\text{mm}$ and $\lambda = 5\text{mm}$. First, in order to check that the flow remains attached along the airfoil chord upstream of the trailing edge, the smoke wand is located upstream of the airfoil leading edge.

This is so that the smoke should follow the boundary layer on both pressure and suction sides and merge at the trailing edge. This is verified in Figure 12*a*, confirming that the flow is attached on pressure and suction sides. In order to study the flow in the close vicinity of the serration, the smoke wand was placed on the pressure side of the airfoil, in the boundary layer upstream of the trailing edge, so that no smoke is generated on the suction side of the airfoil (see Figure 12*b*). Note that the smoke wand was positioned further enough from the trailing edge not to disturb the flow past the trailing edge. Figure 12*c* shows the flow past a straight edge, where smoke is exclusively originating from the pressure side and leaves the airfoil surface tangentially to follow the airfoil wake. By contrast, Figure 12*d* shows the flow leaving the serrated edge with the smoke wand on the pressure side. Part of the flow is forced through the sawtooth troughs, starting from the root of the serrations, where locally the wake begins to mix. This cross flow phenomenon is believed to be the reason for the noise increase at high frequencies when using sawtooth serrated trailing edges.

The reason for this cross flow is suspected to be two fold. First, at the root of the serration the wake starts mixing. Secondly, at the trailing edge, the pressure difference responsible for the noise radiation is sucking air from the pressure side, partly creating this cross flow effect which then develops in the wake along the edges of the sawteeth.

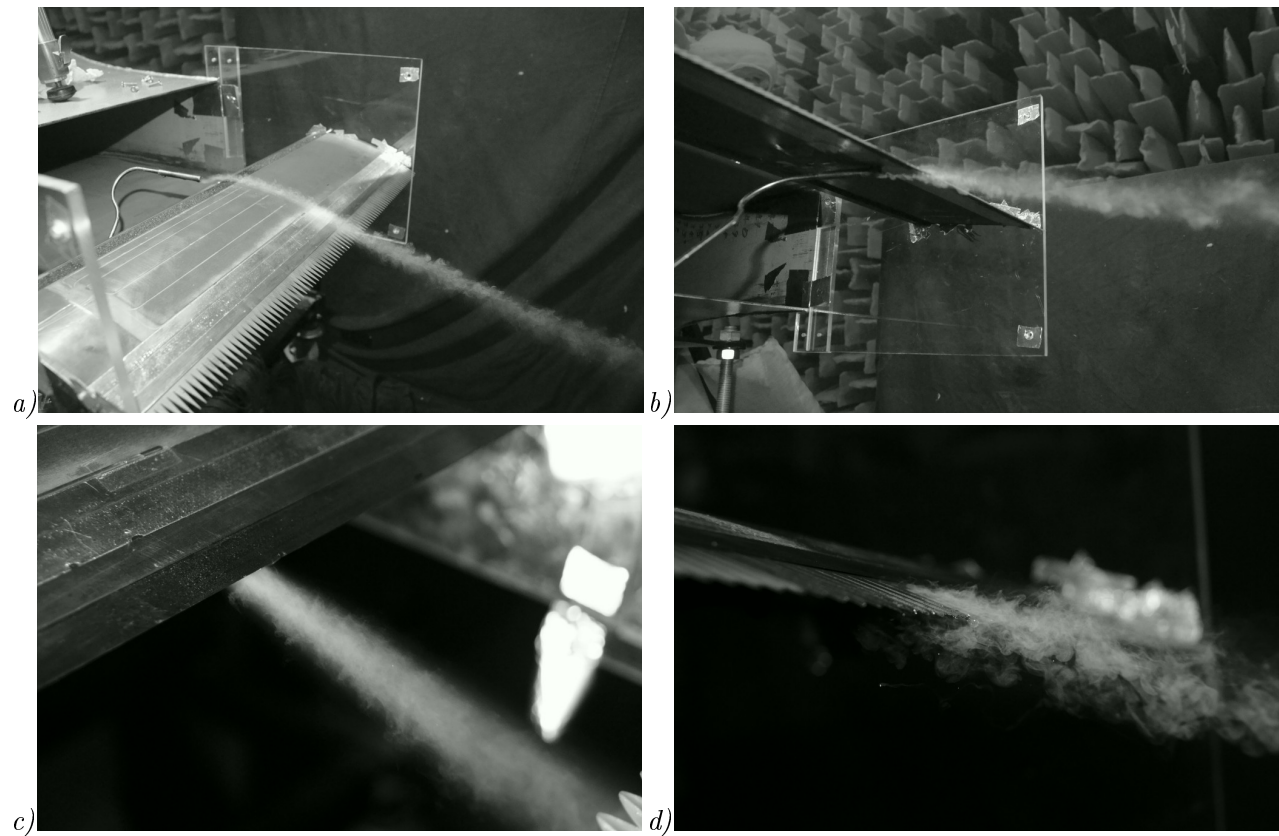


Figure 12. Flow visualisation smoke around a sawtooth serrated trailing edge - (a) Flow around the airfoil, (b) Smoke wand on the pressure side of the airfoil, (c) Flow past a straight edge at 5° AoA, (d) Flow past a sawtooth serrated edge at 5° AoA.

B. Variation of the boundary layer and wake velocity spectra with mean flow velocity

As mentioned previously, the cross flow phenomenon observed in Section A is believed to be the cause of the high frequency noise radiation increase due to sawtooth trailing edges. In order to confirm this hypothesis, this section verifies that the turbulence is increased at the same frequencies at which the noise is increased, i.e., $f\delta/U_0 > 1$.

Measurements of the flow over the airofil trailing edge serration were performed using a single hot wire probe, at $U_0 = 20m/s$ and also for a flow velocity blowdown, where hot wire data is acquired as the mean flow velocity is decreased from $U_0 = 40m/s$ to zero. Data were recorded at 5° angle of attack and for a serration with $2h = 20mm$ and $\lambda = 5mm$. Figure 14 shows $\Delta S_{uu,w}$ in the wake and $\Delta S_{uu,bl}$ in the boundary layer as defined in Equation 5.

$$\Delta S_{uu,w} = 10 * \log 10 \left(\frac{S_{uu,serr,1}}{S_{uu,ref}} \right) \quad \text{and} \quad \Delta S_{uu,bl} = 10 * \log 10 \left(\frac{S_{uu,serr,2}}{S_{uu,ref}} \right), \quad (5)$$

where $S_{uu,serr,1}$ is the streamwise velocity spectrum measured in the wake of a sawtooth serrated trailing edge, in between two sawteeth, $S_{uu,serr,2}$ is the streamwise velocity spectrum measured in the boundary layer over a single sawtooth and $S_{uu,ref}$ is the streamwise velocity spectrum measured in the boundary layer over a straight edge baseline airfoil, as marked in Figure 13. All measurements were taken at the same chordwise distance of $0.15m$ and the same distance from the airfoil surface of about $\delta/2$.

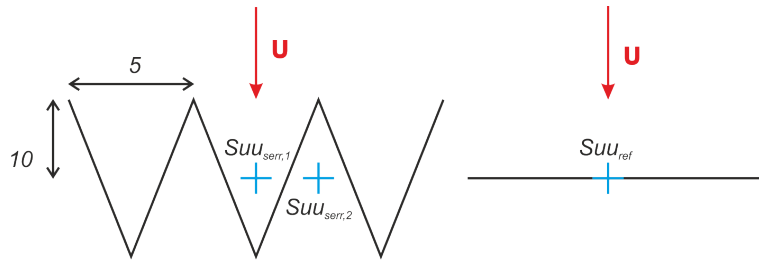


Figure 13. Hot wire measurement locations shown by crosses, (*Left*) Sawtooth trailing edge, (*Right*) Straight reference trailing edge.

Figure 14a shows that $\Delta S_{uu,w}$ follows the same Strouhal number dependence as the noise radiation presented in Section V, with $St_\delta = 1.1$, i.e., the turbulence is increased when $St_\delta > 1$ and the turbulence is decreased when $St_\delta < 1$. Figure 14b shows that $\Delta S_{uu,bl}$ varies very little ($\pm 0.5 dB$) between the straight edge case and the serrated edge case. Comparing these Figures 14a and b indicates that the noise radiation increase due to the introduction of sawtooth serrations is strongly linked to the behaviour of the turbulence in the wake and in the boundary layer.

In addition, Figure 14c also shows the velocity spectrum in the boundary layer over the straight edge, compared to that of the boundary layer over a single sawtooth and that of the very near wake in between two sawteeth, at $U_0 = 20m/s$. The velocity spectrum has a very similar shape to that of the sawtooth boundary layer.

Generally, the behaviour of the velocity spectrum, while moving along the airfoil chord, past the trailing edge and in the wake, has been investigated, but for brevity not shown here. As the

hot wire was traversed along the airfoil suction side towards the trailing edge, the low frequencies of the velocity spectrum increase and the high frequencies decrease due to adverse pressure gradients. While passing into the wake, the velocity spectrum shape remains unchanged but lower in value. This analysis reveals that none of the behaviour pointed above in Figure 14 has been observed over a straight edge, and confirms that the high frequency noise increase is due to increased turbulence activity in between the sawteeth.

Finally, Figures 14a and c also show that the turbulence in the troughs of the sawtooth is reduced by a maximum of about 3 dB for $f\delta/U_0 < 1$ over a large range of mean flow velocities, hence exhibiting roughly the same levels of reduction as the noise (see Figures 14c and d). However, as mentioned above, the turbulence reduction at low frequencies was observed to be due to the flow expanding in the wake, past a straight edge. Therefore, this turbulence reduction in Figures 14a and c is not believed to be a main mechanism in the trailing edge noise reduction due to sawtooth serrations.

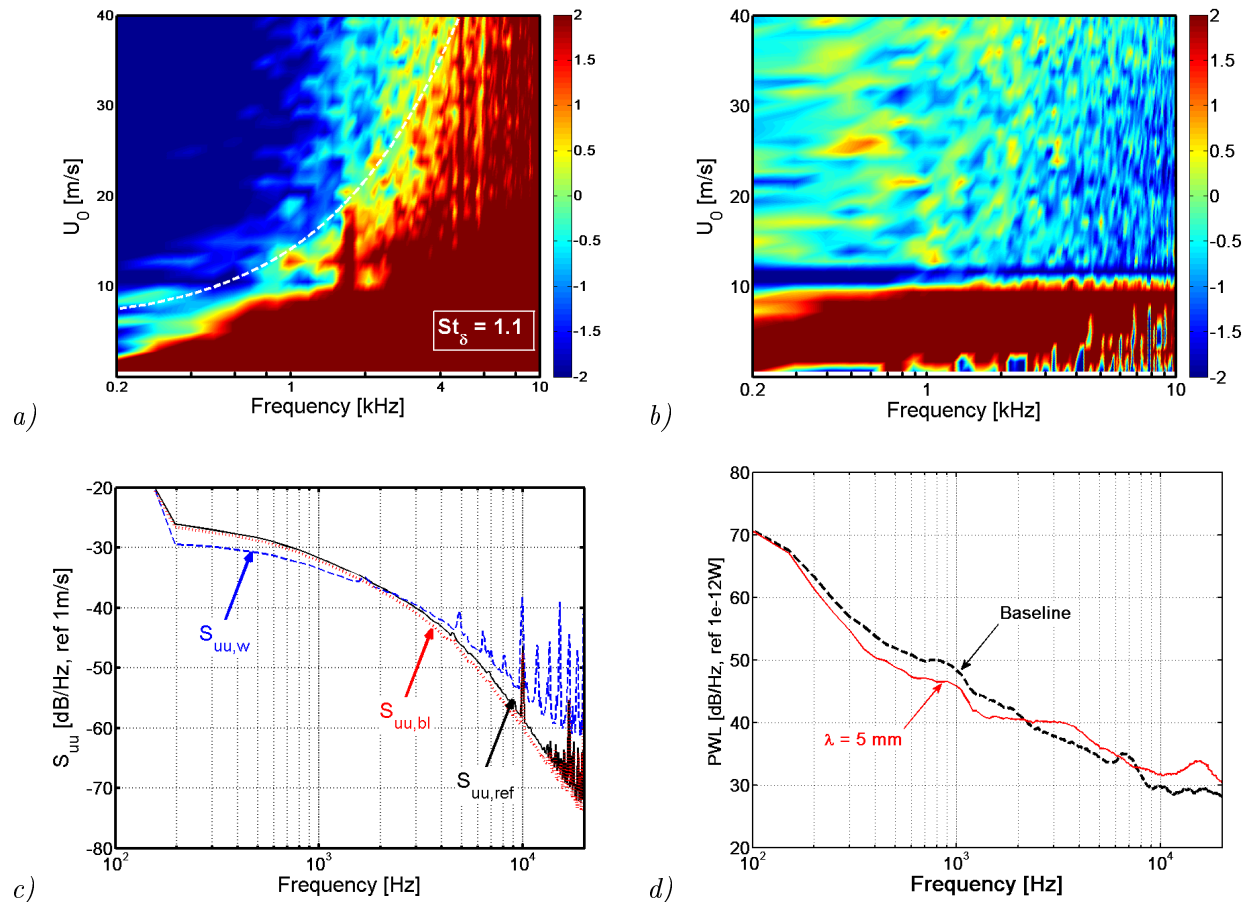


Figure 14. (a) $\Delta S_{uu,w}$ as defined in Equation 5, (b) $\Delta S_{uu,bl}$ as defined in Equation 5, (c) $S_{uu,ref}$ (Solid black), $S_{uu,serr,1}$ (Dotted red) and $S_{uu,serr,2}$ (Dashed blue) measured at 5° AoA and $U_0 = 20 \text{ m/s}$, (d) Corresponding sound power PWL.

VII. Noise mechanisms discussion

In this, and various other studies, serrated trailing edges have been investigated experimentally and analytically as a means of reducing the self noise from airfoils. However, apart from Howe's analytical work, no experimental studies have been performed aimed at understanding the mechanisms involved in achieving noise reductions. Based on the results described in Section IV and V of this paper, this mechanism is discussed. As presented in Section II, Howe introduces three parameters that control the predicted noise reduction, i.e., $\omega\delta/U_c$, h/δ and h/λ . To allow direct comparison with Howe's predictions, the noise reduction mechanism will be discussed in terms of these three parameters below.

- $\omega\delta/U_c$

Frequency defined in terms of Strouhal number with respect to δ has been shown to be a more critical parameter than predicted by Howe. One of the most striking features arising from our investigation is a clear increase in noise at frequencies, $f\delta/U_0 > 1$. This behaviour was not observed in the difference in the turbulent boundary layers between a straight edge and a serrated edge, suggesting that the cause of this high frequency increase is the presence of small jets due to cross-flow through the roots of the sawteeth. At lower frequencies, $f\delta/U_0 < 1$, noise reductions are observed whose level depends on h/λ and h/δ .

- h/δ

The other important observation resulting from our investigation, in addition to the dependence on $f\delta/U_0$, is that insignificant noise reductions were obtained across the entire frequency range for $h/\delta < 0.5$, i.e., when the typical eddy size is larger than the sawtooth amplitude h . In this case the eddies pass over the serration and scattered into sound with an efficiency similar to that of a straight edge. It is also noteworthy that the oscillations in the spectrum predicted by Howe for $h/\delta \approx 1$ arising from coherent interference between the radiation from the root and the tip are not present in the measurements. This suggests that the turbulence at the root and at the tip is largely uncorrelated.

- h/λ

In our experimental investigation, noise reductions from the trailing edge serration were found to improve as h/λ increases, as predicted by Howe. Nevertheless, experimental reductions were substantially smaller than that predicted. However, we have observed that noise reductions are considerably more sensitive to h , through the ratio h/δ , than Howe predicted. For a given h , the noise reduction is equally sensitive to λ as h is for a given value of λ . At the present it is unclear whether h/λ is the independent parameter determining the level of noise reduction, i.e., the angle of the flow relative to the edge, as predicted by Howe, or whether it is λ and h individually.

VIII. Conclusion

This paper reports an experimental study aimed at reducing trailing edge noise using a wide range of over 30 geometries of sawtooth serrated edges on a NACA651210 airfoil. It is shown that

noise reduction of up to 7 dB is achieved over a wide frequency range, while noise is increased at higher frequencies by up to about 3 dB. The increase in noise presents a downside to the use of serrated edges as a means of noise reduction in real applications such as for example aircraft engines, aircraft wings, wind turbine and cooling fan blades. Understanding the reasons for noise reduction and noise increase are of great importance to maximise the noise reduction while minimising the noise increase for a specific application. The experimental results, alongside with the critical comparison with Howe's predictions, show that the following conditions need to be fulfilled to reduce the noise: $f\delta/U_0 < 1$, $h/\delta > 0.5$, and λ to be small. Finally, a discussion on the noise mechanisms involved in the noise reduction is presented. This paper gives the necessary parameters required to design and implement trailing edge sawtooth serration as a means of noise reduction for a specific application.

Acknowledgments

This work was supported by the 7th Framework European Project FLOCON: Adaptive and Passive Flow Control for Fan Broadband Noise Reduction, and Rolls Royce plc.

References

- ¹RK Amiet. Noise due to turbulent flow past a trailing edge. *Journal of Sound and Vibration*, 47(3):387–393, 1976.
- ²TF Brooks and TH Hodgson. Trailing edge noise prediction from measured surface pressures. *Journal of Sound Vibration*, 78:69–117, 1981.
- ³TP Chong, PF Joseph, and P. Davies. A Parametric Study of Passive Flow Control for a Short, High Area Ratio 90 deg Curved Diffuser. *Journal of Fluids Engineering*, 130:111104, 2008.
- ⁴TP Chong, PF Joseph, and P. Davies. Design and performance of an open jet wind tunnel for aero-acoustic measurement. *Applied Acoustics*, 70(4):605–614, 2009.
- ⁵AGM Dassen, R. Parchen, J. Bruggeman, and F. Hagg. Results of a wind tunnel study on the reduction of airfoil self-noise by the application of serrated blade trailing edges . In *Proc. of the European Union Wind Energy Conference and Exhibition, Göteborg*, pages 800–803, 1996.
- ⁶M. Drela. Xfoil- an analysis and design system for low reynolds number airfoils. *Low Reynolds Number Aerodynamics*, pages 1–12, 1989.
- ⁷M. Gruber, M. Azarpeyvand, and P. Joseph. Airfoil trailing edge noise reduction by the introduction of sawtooth and slotted trailing edge geometries. In *20th ICA conference*, 2010.
- ⁸M. Gruber, P. Joseph, and TP. Chong. Experimental investigation of airfoil self noise and turbulent wake reduction by the use of trailing edge serrations. In *16th AIAA/CEAS Aeroacoustics Conference*, 2010.
- ⁹MS Howe. A review of the theory of trailing edge noise. *Journal of Sound and Vibration*, 61(3):437–465, 1978.
- ¹⁰MS Howe. Aerodynamic noise of a serrated trailing edge. *Journal of Fluids and Structures*, 5(1):33–45, 1991.
- ¹¹MS Howe. Noise produced by a sawtooth trailing edge. *The Journal of the Acoustical Society of America*, 90:482, 1991.
- ¹²MS Howe. Trailing edge noise at low Mach numbers. *Journal of Sound and Vibration*, 225(2):211–238, 1999.
- ¹³S. Oerlemans, M. Fisher, T. Maeder, and K. Kögler. Reduction of wind turbine noise using optimized airfoils and trailing-edge serrations. *AIAA journal*, 47:1470–1481, 2009.
- ¹⁴R. Parchen, W. Hoffmans, A. Gordner, and K. Braun. Reduction of airfoil self-noise at low Mach number with a serrated trailing edge. In *International Congress on Sound and Vibration, 6 th, Technical Univ. of Denmark, Lyngby, Denmark*, pages 3433–3440, 1999.

¹⁵J.E.F. Williams and LH Hall. Aerodynamic sound generation by turbulent flow in the vicinity of a scattering half plane. *Journal of Fluid Mechanics*, 40(04):657–670, 1970.